

Effect of the gain model on the stability map of optically injected DFB lasers

Ivan Aldaya^a, Gabriel Campuzano^a, Christophe Gosset^b,
Cheng Wang^b, Frederic Grillot^b, and Gerardo Castañón^a

^aTecnológico de Monterrey, Garza Sada Av. 2501, 64849, Monterrey, Mexico;

^bTelecom ParisTech CNRS LTCI, 46 Rue Barrault, 75634, Paris, France

ABSTRACT

Optical injection locking of semiconductor lasers has attracted significant attention due to its applications in laser analysis, modulation characteristic enhancement, and nonlinear dynamics. In many cases, the analysis of the optically injected laser is done by simulation, requiring an accurate laser model and, therefore, an adequate modeling of the gain compression at high photon densities. We use the Kobayashi-Lang rate equations to numerically compare the stable locking range considering four different gain models. Results reveal that at low bias currents, gain compression is significant only under weak injection regime. In contrast, for higher bias current, gain compression must be considered both in weak and strong injection regimes.

Keywords: optical injection locking, gain model, laser simulation.

1. INTRODUCTION

Optical gain compression was a matter of research since the early days of the development of semiconductor lasers.¹⁻³ In multimode lasers, gain compression results in intermodal gain, explaining the spectral asymmetry observed experimentally. In single mode lasers, such as distributed feedback (DFB) lasers, gain saturation at high photon densities must be considered in order to explain several phenomena. On the one hand, gain compression is the major factor contributing to the damping of the resonance frequency⁴ and, on the other hand, it is required to correctly model the adiabatic chirp.⁵ It is commonly accepted that the main physical mechanism responsible for this gain compression is the finite intraband relaxation time induced by hole burning.^{4,6,7} In contrast to gas and solid state lasers, where gain compression was addressed theoretically using the density matrix formalism, in semiconductor lasers, gain compression has been usually included in a phenomenological approach.⁸ In this way, different gain models has been proposed to match experimental results:⁷ the simplest nonlinear gain model includes a power dependent gain-suppression, being the optical gain modeled as $G = G_N(N - N_{tr}) - G_S S$, where G_N is the differential gain, N is the carrier density, N_{tr} is the transparency carrier density, and G_S and S are the derivative of the gain with respect to the photon density and the photon density, respectively.⁹ This model is valid for low photon densities but at higher photon densities, it does not accurately model the laser dynamics. A more realistic model for optical gain includes a multiplicative gain compression term, $G = (1 - \epsilon_A S)^{-1} G_N(N - N_{tr})$, with ϵ_A the gain compression parameter. This approximation model a two-level laser but it is not correct for semiconductor lasers where transitions occur between energy bands. Agrawal proposed a new gain model derived using density matrix formalism, yielding to $G = (1 - \epsilon_B S)^{-1/2} G_N(N - N_{tr})$, being ϵ_B the gain compression parameter of the model.^{7,8} In this work, we will compare the resulting stability range for the four gain models:

- Linear gain: $G_{linear} = G_N(N - N_{tr})$
- Nonlinear gain model 1: $G_{NL1} = G_N(N - N_{tr}) - G_S S$
- Nonlinear gain model 2: $G_{NL2} = (1 + \epsilon_A S)^{-1} G_N(N - N_{tr})$
- Nonlinear gain model 3: $G_{NL3} = (1 + \epsilon_B S)^{-1/2} G_N(N - N_{tr})$

Reference	Year	Gain model	Injection regime
Lang ¹³	1982	G_{linear}	Strong
Mogensen <i>et al.</i> ¹⁴	1985	G_{linear}	Strong
Lidoynes <i>et al.</i> ⁹	1990	G_{NL1}	Weak
Lidoynes <i>et al.</i> ¹¹	1991	G_{NL1}	Weak
Hui <i>et al.</i> ¹⁵	1991	G_{NL1}	Weak
Hui <i>et al.</i> ¹⁶	1991	G_{NL1}	Weak
Mohrdiek <i>et al.</i> ¹²	1994	G_{NL2}	Strong
Yabre <i>et al.</i> ¹⁷	1996	G_{NL1}	Medium
Yabre <i>et al.</i> ¹⁸	1997	G_{NL1}	Medium
Wieczorek <i>et al.</i> ¹⁰	2005	G_{linear}	Strong
Lau ¹⁹	2006	G_{linear}	Strong
Lau <i>et al.</i> ²⁰	2009	G_{linear}	Strong
Stolz <i>et al.</i> ²¹	2010	G_{linear}	Strong
Parekh ²²	2012	G_{linear}	Strong

Table 1. Gain models used in literature.

Gain compression in weakly injected lasers has been studied in,¹¹ demonstrating that gain compression is required to obtain a locking map consistent with experimental observations. However, at strong injection regime, gain compression is generally neglected adducing that linear gain model is accurate enough.¹⁰ Nevertheless, even at high injection ratios, gain compression damps the resonance frequency and, in consequence, it affects the stability of the injected laser, resulting in a locking map. Table 1 lists some of the previous analytical works, indicating the employed gain model and the injection regime. For weak (and medium) injection regime, Lidoyne *et al.*¹¹ compared the obtained locking map using G_{linear} and G_{NL1} , showing that it is necessary to include gain compression at weak injection ratios. The present work considers both weak and strong injection regimes, to study the impact of the gain model not only under weak injection but also at stronger injection ratios, where, with the exception of,¹² G_{linear} has been the only employed gain model.

The objective of this paper is to compare the different gain models (the linear model and the three nonlinear gain models) in order to clarify whether it is necessary to consider gain compression. In addition, we analyze whether more complicated gain compression model adds a significant difference compared to the simplest gain compression model. The paper is divided as follows: in Section 2 the relation among the different gain compression parameters are derived. In Section 3 the small signal analysis is presented, which requires the linearization of the Kobayashi-Lang rate equations for the different gain models. Numerical results are presented in Section 4 and, finally, Section 5 concludes the paper.

2. NONLINEAR GAIN MODELS

Gain compression in G_{NL1} is usually introduced as a subtraction, but it can be alternatively represented as a multiplicative term:

$$G_{NL1} = G_N(N - N_{tr}) - G_S S = (1 - \epsilon S)G_N(N - N_{tr}) \quad (1)$$

Further author information:

Gabriel Campuzano: E-mail: campuzano@itesm.mx

with $G_S = \epsilon G_N(N - N_{tr})$, being ϵ the new compression parameter. For low photon densities, $\epsilon_A S \ll 1$, G_{NL2} can be approximated by:

$$G_{NL2} = \frac{G_N(N - N_{tr})}{1 + \epsilon_A S} \approx G_N(N - N_{tr}) - \epsilon_A G_N(N - N_{tr})S = (1 - \epsilon_A)G_N(N - N_{tr}). \quad (2)$$

By inspection we get that $\epsilon_A = \epsilon$, which is further related to G_S through Eq. 1. Operating in the same way for G_{NL3} we get an approximated expression:

$$G_{NL3} = \frac{G_N(N - N_{tr})}{\sqrt{1 + \epsilon_B S}} \approx G_N(N - N_{tr}) - \frac{1}{2}\epsilon_B G_N(N - N_{tr})S \quad (3)$$

and, consequently, $\epsilon_A = \frac{1}{2}\epsilon_B$. Table 2 summarizes the relations among G_S , ϵ_A , and ϵ_B .

Parameter	G_S	ϵ_A	ϵ_B
G_S	-	$\epsilon_A G_N(N - N_{tr})$	$\epsilon_B G_N(N - N_{tr})/2$
ϵ_A	$G_S/(G_N(N - N_{tr}))$	-	$\epsilon_B/2$
ϵ_B	$2G_S/(G_N(N - N_{tr}))$	$2\epsilon_A$	-

Table 2. Relation between the gain compression parameters of the different models.

The different gain models are compared in Fig. 1. In Fig. 1(a) the gain multiplicative term is represented in terms of the photon density, S . At low S densities, the different gain models converge, in accordance to,⁷ but for higher values of S , G_{NL1} reduces excessively the gain and therefore, it overestimates the damping factor. Figure 1(b) shows the derivative of the gain with respect to S . It is obvious that for G_{NL1} the derivatives is constant in contrast to G_{NL2} and G_{NL3} whose derivatives depend on S . It is important to note that the main difference appears between G_{NL1} and the other two nonlinear models, whereas there is not a significant difference between G_{NL2} and G_{NL3} .

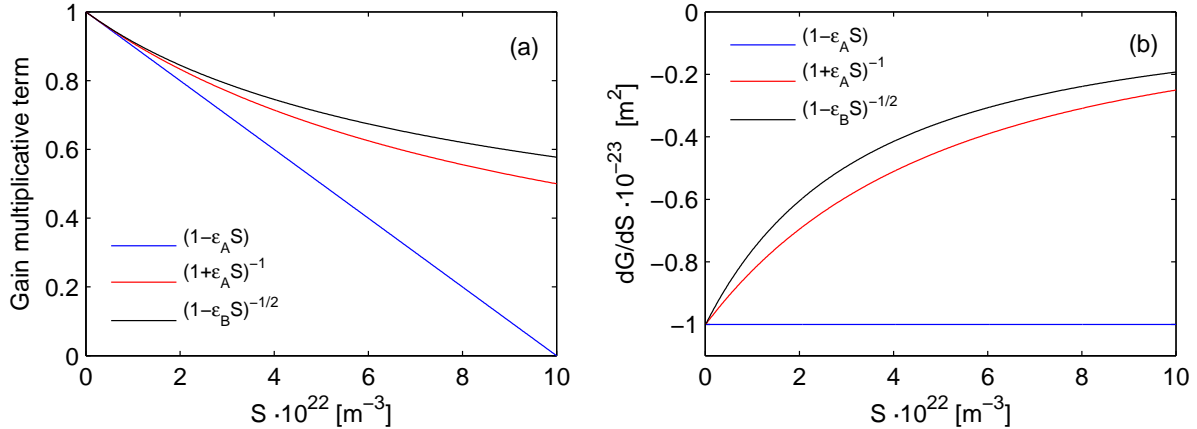


Figure 1. Comparison of the different gain models for $\epsilon_A = 10^{-23}m^3$ as a function of the photon density, S : (a) gain multiplicative term and (b) differential gain with respect to S .

3. STABILITY ANALYSIS

In optically injected lasers, stability analysis is a critical point. Stability analysis is performed using the well-known small-signal analysis, where first the steady state solution is found and, afterwards, a small sinusoidal signal is applied. The system is stable if, after the perturbation, it returns to the steady state. Given the small-signal nature of the applied signal, the system can be linearized around the steady state solution and

	G_{linear}	G_{NL1}	G_{NL2}	G_{NL3}
m_{SS}	z'	$z' + 2G_S S_0$	$\gamma_P - \frac{\gamma_P - 2z'}{(1 + \epsilon_A S_0)^2} - z'$	$\gamma_P - \frac{\gamma_P - 2z'(1 + \frac{1}{2}\epsilon_B S_0)}{(1 + \epsilon_B S_0)^{3/2}} - z'$
$m_{S\phi}$	$2S_0 z''$	$2S_0 z''$	$2S_0 z''$	$2S_0 z''$
m_{SN}	$-G_N S_0$	$-G_N S_0$	$-\frac{G_N}{1 + \epsilon_A S_0} S_0$	$-\frac{G_N}{(1 + \epsilon_B S_0)^{1/2}} S_0$
$m_{\phi S}$	$-\frac{z''}{2S_0}$	$-\frac{z''}{2S_0}$	$-\frac{z''}{2S_0}$	$-\frac{z''}{2S_0}$
$m_{\phi\phi}$	z'	z'	z'	z'
$m_{\phi N}$	$-\frac{\alpha}{2} G_N$	$-\frac{\alpha}{2} G_N$	$-\frac{\alpha}{2} G_N$	$-\frac{\alpha}{2} G_N$
m_{NS}	$\gamma_P - 2z'$	$\gamma_P - 2z' - 2G_S S_0$	$\frac{\gamma_P - 2z'}{(1 + \epsilon_A S_0)^2}$	$\frac{\gamma_P - 2z'(1 + \frac{1}{2}\epsilon_B S_0)}{(1 + \epsilon_B S_0)^{3/2}}$
$m_{N\phi}$	0	0	0	0
m_{NN}	$\gamma_N + G_N S_0$	$\gamma_N + G_N S_0$	$\gamma_N + \frac{G_N S_0}{1 + \epsilon_A S_0}$	$\gamma_N + \frac{G_N S_0}{(1 + \epsilon_B S_0)^{1/2}}$

Table 3. Linearized terms for the different gain models.

stability can be assessed using Routh-Kurwitz criterion, which estabes that in order to be stable all the zeros of the characteristic determinant must be located in the negative half of the s-plane.¹⁴

The rate equations governing the optically injected laser are known as Lang-Kobayashi equations.^{13,14} This set of coupled rate equations are the conventional laser rate equations for photon density, S , phase, ϕ , and carrier density, N , modified to include the injected field:

$$\frac{d}{dt}S(t) = [G(N, S) - \gamma_P]S(t) + \kappa\sqrt{S_{inj}S(t)}\cos(\phi_L) \quad (4a)$$

$$\frac{d}{dt}\phi(t) = \frac{1}{2}\alpha[G_N(N - N_{tr}) - \gamma_P] + \kappa\sqrt{\frac{S_{inj}}{S(t)}}\sin(\phi_L) \quad (4b)$$

$$\frac{d}{dt}N(t) = J - \gamma_N N(t) - G(N, S)S(t) \quad (4c)$$

where $G(N, S)$ is the optical gain that depends on both N and S , γ_P stands for the internal optical losses, κ is the injection efficiency, S_{inj} is the injected photon density, and ϕ_L is the phase difference between the emitted field and the injected field. α is the linewidth enhancement factor accounting for the coupling between the imaginary and real parts of the refractive index in the active region. J is the injected carrier density and γ_N is the equivalent carrier decay rate. Gain compression does not appear in Eq. 4b because the gain saturation induced by hole burning is symmetrical around the emission frequency.¹¹

A detailed method to find the steady state solutions is presented in.¹⁹ The method requires to set the locking phase, ϕ_L , and the power injection ratio, ρ . After some algebra, a cubic equation is yield for the static field amplitude, A_0 , which is related to the static photon density, S_0 through $S_0 = A_0^2$.

$$A_0^3 - \left(\frac{2\kappa}{\gamma_P}A_{inj}\cos(\phi_L)\right)A_0^2 - A_{fr}A_0 - \frac{\gamma_N 2\kappa}{\gamma_P G_N}A_{inj}\cos(\phi_L) = 0, \quad (5)$$

where A_{inj} is the amplitude of the injected field given by $A_{inj} = \sqrt{S_{inj}}$.

The power injection ratio, ρ , and the normalized injection ratio, z , are defined as:

$$\rho = \frac{S_{inj}}{S_0} \text{ and } z = \kappa\sqrt{\frac{S_{inj}}{S_0}}. \quad (6)$$

For the sake of simplicity in future calculations, it is useful to define:

$$z' = z \cdot \cos(\phi_L) \text{ and } z'' = z \cdot \sin(\phi_L) \quad (7)$$

Laser parameter	Symbol	Value	Units
Emission wavelength	λ_0	1550	nm
Differential gain	G_N	5667	s ⁻¹
Threshold carrier density	N_{th}	$2.21 \cdot 10^8$	m ⁻³
Photon decay rate	γ_P	$0.33 \cdot 10^{-12}$	s ⁻¹
Electron decay rate	γ_N	10^{-9}	s ⁻¹
Coupling efficiency	κ	$183 \cdot 10^{-9}$	s
Linewidth enhancement factor	α	3	
Threshold current	I_{th}	10	mA
Gain compression parameter	ϵ	10^{-23}	m ³

Table 4. Laser parameters for numerical stability analysis.

The frequency detuning between the injected and the free-running laser field, $\Delta\omega$, can be calculated in terms of z and the locking phase ϕ_L through the expression:

$$\Delta\nu = -\frac{1}{2\pi}z\sqrt{1+\alpha^2}\sin(\phi_L + \text{atan}(\alpha)) \quad (8)$$

Once the steady state solutions are found, the rate equations are linearized around the static operation point. At this point gain compression comes into play, since the linearized terms are dependent on the gain model. The linearized system is usually expressed in matrix form as:

$$\begin{pmatrix} m_{SS} + s & m_{S\phi} & m_{SN} \\ m_{\phi S} & m_{\phi\phi} + s & m_{\phi N} \\ m_{NS} & m_{N\phi} & m_{NN} + s \end{pmatrix} \cdot \begin{pmatrix} \delta S \\ \delta\phi \\ \delta N \end{pmatrix} = \begin{pmatrix} F_S \\ F_\phi \\ F_N \end{pmatrix} \quad (9)$$

where F_S , F_ϕ , and F_N are the Langevin forces for the photon density, field phase, and carrier density, respectively, and m_{XX} are the linearized elements shown in Table 2. δS , $\delta\phi$, and δN are the perturbations and s is the complex frequency variable. As can be seen in Table 2, m_{SS} , m_{SN} , m_{NS} , and m_{NN} depend on the gain model and therefore, they affect the system stability.

4. NUMERICAL RESULTS

Table 4 presents the laser parameters employed in the numerical analysis, which are typical for a multi quantum well DFB laser.²⁰ In²⁰ gain compression is not considered so we used the gain compression reported in.⁶

Figures 2 and 3 show the locking map for bias currents corresponding to 5 and 10 times the threshold current (I_{th}), respectively. For each case, the locking map is presented in (a) the phase plane and (b) in the ρ vs. $\Delta\nu$ plane. In Fig. 2(a), it can be seen that the difference between the dynamic boundaries obtained with and without considering gain compression, is only significant at low ρ values. Furthermore, all the three gain compression models result in indistinguishable dynamic boundaries. This is translated to a ρ vs. $\Delta\nu$ locking map, Fig. 2(b), where the difference between gain models (linear and nonlinear models) is only appreciable at weak injection regime, inset in Fig. 2(a), in accordance with experimental results presented in.¹¹ For higher bias currents, $10I_{th}$, numerical results reveal a slightly different behavior. First of all, when linear gain is considered, the resulting dynamic boundary is significantly underestimated compared to gain models where gain compression is taken into account, Fig. 3(a). Furthermore, in Fig. 3(a), a slight difference between G_{NL1} and the other two nonlinear gain models can be seen for low ρ values. This difference is clearer in the inset of Fig. 3(b). Hence, G_{NL1} slightly overestimates the stable locking range when compared with G_{NL2} and G_{NL3} , which are indistinguishable. This

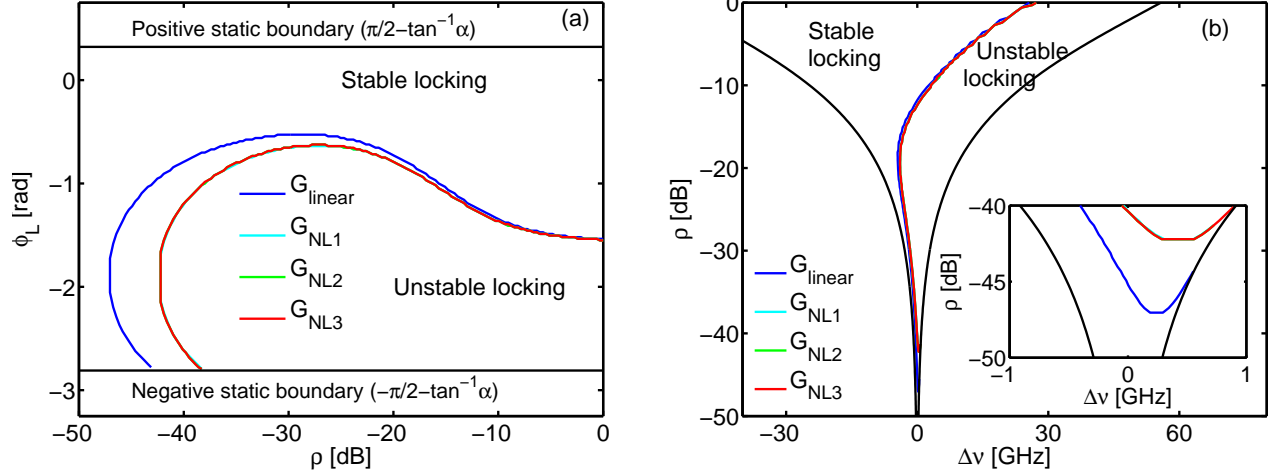


Figure 2. Locking diagrams for $I = 5I_{th}$ in (a) the phase plane and (b) the ρ vs. $\Delta\nu$ plane, the inset shows the locking map for low power injection ratios.

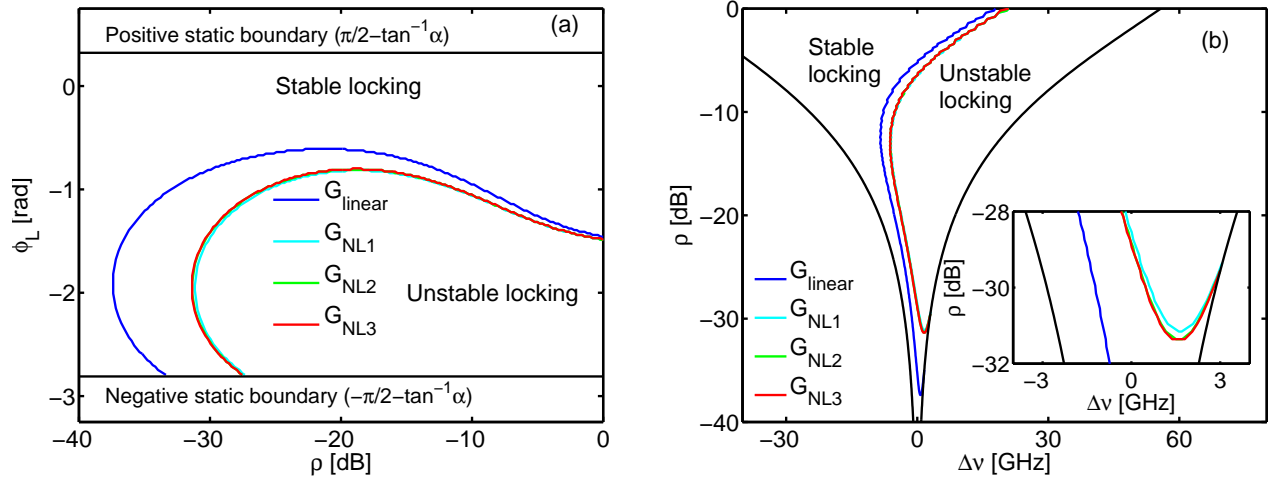


Figure 3. Locking diagrams for $I = 10I_{th}$ in (a) the phase plane and (b) the ρ vs. $\Delta\nu$ plane, the inset shows the locking map for low power injection ratios.

is consistent with Fig. 1(a): at low bias currents, i.e. low photon densities, the different gain models converge, whereas at higher bias currents, i.e. higher photon densities, G_{NL1} diverges from G_{NL2} and G_{NL3} , which remain relatively close. For stronger ρ levels, the difference among G_{NL1} , G_{NL2} , and G_{NL3} is not significant anymore but, in contrast to what occurred for lower bias current, there is still a difference between the dynamic boundaries corresponding to linear and nonlinear gain models.

5. CONCLUSIONS

In this paper, the stability of DFB lasers subject to injection has been numerically studied for different gain models. The relations among the gain compression parameters of the different gain models have been derived and the Kobayashi-Lang equations have been linearized considering the different gain models. Numerical results show that at low bias currents gain compression is only significant at weak injection regime, but at higher bias currents, gain compression should be considered both in weak and strong injection. In regards with the gain model accuracy, although from a theoretical point of view G_{NL3} is more realistic than G_{NL1} and G_{NL2} , G_{NL3} results in similar dynamic boundary to G_{NL2} and G_{NL1} even for high bias currents. In consequence, G_{NL1} shows a good tradeoff between simplicity and accuracy.

REFERENCES

1. Furuya, K., Suematsu, Y., Sakakibara, Y., and Yamada, M., "Influence of intraband electronic relaxation on relaxation oscillation of injection laser," *Transactions of IECE* **62**, 241–245 (Apr. 1979).
2. Adams, M. J. and Osinski, M., "Influence of spectral hole-burning on quaternary laser transients," *IEEE Electronics Letter* **19**, 627–628 (Aug. 1983).
3. Channin, D. J., "Effect of gain saturation on injection laser switching," *Journal of Applied Physics* **50**, 3858–3860 (Jun. 1979).
4. Buus, J., [*Single frequency semiconductor lasers*], vol. TT5, SPIE Optical Engineering Press, Bellingham, Washington USA, 1st ed. (1990).
5. Bjerkan, L., Royset, A., Hafskjaer, L., and Myhre, D., "Measurement of laser parameters for simulation of high-speed fiberoptic systems," *Journal of Lightwave Technology* **14**, 839 – 850 (May 1996).
6. Carroll, J., Whiteaway, J., and Plumb, D., [*Distributed feedback semiconductor lasers*], IET (1998).
7. Agrawal, G., "Effect of gain and index nonlinearities on single-mode dynamics in semiconductor lasers," *IEEE Journal of Quantum Electronics* **26**, 1901–1909 (Nov. 1990).
8. Agrawal, G., "Gain nonlinearities in semiconductor lasers: theory and application to distributed feedback lasers," *IEEE Journal of Quantum Electronics* **23**, 860 – 868 (Jun. 1987).
9. Lidoyne, O., Gallion, P., Chabran, C., and Debarge, G., "Locking range, phase noise and power spectrum of an injection-locked semiconductor laser," *Optoelectronics, IEE Proceedings J* **137**, 147–154 (Jun 1990).
10. Wiczoreka, S., Krauskopf, B., Simpson, T., and Lenstra, D., "The dynamical complexity of optically injected semiconductor lasers," *Elsevier Physics Reports* (2005).
11. Lidoyne, O., Gallion, P., and Erasme, D., "Modulation properties of an injected semiconductor laser," *IEEE Journal of Quantum Electronics* **27**, 344–351 (Mar. 1991).
12. Mohrdiek, S., Burkhard, H., and Walter, H., "Chirp reduction of directly modulated semiconductor lasers at 10 Gb/s by strong CW light injection," *Journal of Lightwave Technology* **12**, 418 – 424 (Mar. 1994).
13. Lang, R., "Injection locking properties of a semiconductor laser," *IEEE Journal of Quantum Electronics* **18**, 976 – 983 (Jun. 1982).
14. Mogensen, F., Olesen, H., and Jacobsen, G., "Locking conditions and stability properties for a semiconductor laser with external light injection," *IEEE Journal of Quantum Electronics* **21**, 784–793 (Jul. 1985).
15. Hui, R., D'Ottavi, A., Mecozzi, A., and Spano, P., "Injection locking in distributed feedback semiconductor lasers," *IEEE Journal of Quantum Electronics* **27**(6), 1688–1695 (1991).
16. Hui, R., Mecozzi, A., D'Ottavi, A., and Spano, P., "Novel measurement technique of α factor in DFB semiconductor lasers by injection locking," *IEEE Electronics Letter* **26**, 997 – 998 (Jul. 1990).
17. Yabre, G., "Effect of relatively strong light injection on the chirp-to-power ratio and the 3 dB bandwidth of directly modulated semiconductor lasers," *Journal of Lightwave Technology* **14**, 2367 – 2373 (Oct. 1996).
18. Yabre, G. and Le Bihan, J., "Reduction of nonlinear distortion in directly modulated semiconductor lasers by coherent light injection," *IEEE Journal of Quantum Electronics* **33**, 1132–1140 (Jul. 1997).
19. Lau, E., *High-Speed Modulation of Optical Injection-Locked Semiconductor Lasers*, PhD thesis, University of California at Berkeley (2006).
20. Lau, E., Wong, L. J., and Wu, M., "Enhanced modulation characteristics of optical injection-locked lasers: a tutorial," *IEEE Journal of Selected Topics in Quantum Electronics* **15**, 618–633 (May 2009).
21. Stolz, C., Labukhin, D., Zakhleniuk, N., and Adams, M., "Dynamics of optically-injected semiconductor lasers using the travelling-wave approach," *IEEE Journal of Quantum Electronics* **46**, 220–227 (Feb. 2010).
22. Parekh, D., *Optical Injection Locking of Vertical Cavity Surface-Emitting Lasers: Digital and Analog Applications*, PhD thesis, University of California at Berkeley (2012).